## Electronic Structure of Liquid Alkanes: A Representative Case of Liquid Hexanes and Cyclohexane Studied Using Polarization-Dependent Two-Photon Absorption Spectroscopy

Dhritiman Bhattacharyya, Yuyuan Zhang, <sup>1</sup>
Christopher G. Elles<sup>2</sup> and Stephen E. Bradforth\*

Department of Chemistry, University of Southern California, Los Angeles, California 90089-0482, USA

#### **Abstract**

Two photon absorption (2PA) spectra of liquid cyclohexane and hexanes are reported for the energy range 7-8.5 eV (177-145nm), providing detailed information on their electronic structures in bulk liquid. Using a broadband pump-probe fashion, the continuous 2PA spectra are measured by simultaneous absorption of a 266 nm (4.6 eV) pump photon and one UV-visible probe photon from the white-light continuum (1.8-3.9 eV). Theoretical one photon absorption (1PA) and 2PA cross sections of isolated gas phase molecules are computed by the equation of motion coupled-cluster method with single and double substitutions (EOM-CCSD) to substantiate the assignment of the experimental spectra, and the natural transition orbital (NTO) analysis provides visualization of the participating orbitals in a transition. Our analysis suggests that, upon solvation, transitions at the lowest excitation energy involving promotion of electron to the 3s Rydberg orbitals are blue-shifted (~0.55 eV for cyclohexane and ~ 0.18 eV for hexanes) to a greater extent as compared to those involving other Rydberg orbitals, that is similar to the behavior observed for water and alcohols. All other transitions experience negligible gas to liquid shift for cyclohexane, whereas these are red-shifted by ~0.15-0.2 eV upon solvation in hexanes. In both alkanes, the spectra are entirely dominated by Rydberg transitions: the most intense bands in 1PA and 2PA spectra are due to the excitation of electrons to the Rydberg 'p' and 'd' type orbitals, respectively, although one transition terminating in the 3s Rydberg has significant 2PA strength. This work demonstrates that the gas phase electronic transition properties in alkanes are not significantly altered upon solvation. In addition, electronic structure calculations using an isolated-molecule framework appear to provide a reasonable starting point for a semi-quantitative picture for spectral assignment and also to analyze the solvatochromic shifts for liquid phase absorption spectra.

<sup>&</sup>lt;sup>1</sup> Current address: Department of Chemistry and Biochemistry, The Ohio State University, 100 West 18th Ave. Columbus OH 43210

<sup>&</sup>lt;sup>2</sup> Current address: Department of Chemistry, University of Kansas, 1567 Irving Hill Road, Lawrence KS 66045

<sup>\*</sup> Corresponding author: stephen.bradforth@usc.edu

#### I. Introduction

Understanding the fate of optically bright Rydberg states in the condensed phase has been a persistent challenge in electronic spectroscopy. Even for an isolated molecule, accurately predicting the shape of the potential energy surface (PES) and the transition dipole moment from electronic structure calculation requires quantifying the coupling between a Rydberg state with other Rydberg or valence states. 1-7 Pioneering work has been carried out by Chergui and coworkers to study Rydberg orbitals in condensed environments. By trapping nitric oxide (NO) molecule in molecular matrices<sup>8-9</sup> and rare gas matrices, <sup>10-11</sup> they showed that optical excitation to a Rydberg state leads to an increase in the spatial distribution of the electrons, giving rise to a large change in the molecule-matrix interaction. The gas-to-matrix shift of transition energies and the broadening of absorption bands depend on the size of the matrix cage and the nature of the Rydberg orbital (s, p, or d type). 12 The dominance of Rydberg excitations was also confirmed in neat benzene and benzene in hexane solution via two-photon fluorescence excitation spectroscopy by Albrecht and coworkers. 13 The local solvation environment has considerable influence on the Rydberg transition properties. For example, the fluorescence lifetime of a molecular Rydberg state in NO is lengthened when going from gas to condensed phase.<sup>14</sup> Furthermore, because of mixing of Rydberg orbitals with the solvent continuum, the characterization of these orbitals below the vertical ionization energy (VIE) provides invaluable information on the competing ionization and dissociation channels. 15-18

Simple saturated sigma-bonded molecular liquids like alkanes and cycloalkanes are ideal systems to investigate the fate of Rydberg transitions in the condensed phase. Since they lack any  $\pi$  electron and low-lying valence excitations, transitions in these molecules are mostly of Rydberg

type. Electronic structure and spectroscopy of these molecules are less explored than their conjugated or aromatic counterparts. For gas phase 1PA spectra of linear alkanes, the Rydberg transitions are not well resolved, even for small chain molecules. 19-21 Cyclic alkanes, on the contrary, show distinct Rydberg transitions, as previously demonstrated for adamantane, cyclopropane, cyclobutane, cyclohexane, bicyclo[2.2.2]octane etc. 22-24 These sharp Rydberg transitions usually rest upon broad featureless continuum, which arises due to the  $\sigma \rightarrow \sigma^*$  type valence transitions. 25 The vibronic features associated with these Rydberg transitions are difficult to interpret and there are only a few examples in the literature that address this issue. 22, 25-26

Raymonda and Simpson adopted independent-systems theory to predict the energy levels of the lower electronic states of an isolated alkane molecule in 1PA.<sup>21</sup> In this method, the C-C bonds are treated separately from the C-H bonds. Starting from the excitation band ( $\sigma_{C-C} \rightarrow \sigma^*_{C-C}$ ) of an ethane monomer unit, the energy levels of higher alkanes can be calculated by introducing the nearest neighbor interactions and breaking the degeneracy. Although this exciton model works surprisingly well for substituted/unsubstituted alkanes and cycloalkanes, it falls short in explaining a weak 1PA band observed in most of the alkanes and specially in branched alkanes in the region between 7-8 eV. Raymonda et al. assigned this band to intramolecular charge transfer between adjacent C-C segments, but this assignment was later refuted by Lombos et. al<sup>20</sup> and Robin<sup>25, 27</sup> who suggested this transition involves electron promotion to Rydberg 3s orbital. One factor that often complicates the analysis of the alkane spectra is the presence of several equilibrium conformations at room temperature. Although the absorption frequencies of different conformers are not expected to deviate much from one another, the oscillator strengths may vary drastically due to the change in molecular point group symmetry that directly determines the transition selection rule.

Spectral analysis becomes further complicated in going from gas to liquid phase, as sharp Rydberg transitions are broadened and overlap with neighboring transitions, giving rise to a featureless spectrum. Just as in the gas phase, alkane and cycloalkanes can exist in several conformations in liquid state. For example, cyclohexane has chair and boat conformations. Molecular dynamics (MD) simulation studies predicted that cyclohexane mainly exists in 'chair' conformation in liquid phase at room temperature.<sup>28</sup> The situation is markedly more complicated for n-hexane, which in principle, can adopt twelve different conformations. Ab-initio and density functional calculations suggest that the lowest energy conformer is all-trans (TTT), which is followed by nearly isoenergetic trans-gauche-trans (TGT) and gauche-trans-trans (GTT) conformers.<sup>29</sup> Further up in energy is trans-gauche-gauche (TGG) conformer.<sup>29</sup> At room temperature, in deuterated liquid hexane, there is almost an equal distribution of all-trans and allgauche conformations present, as predicted by MD simulation and neutron diffraction studies.<sup>30</sup> On the other hand, low frequency isotropic Raman studies predict that ~20% of the conformers are present in all-trans form, whereas ~50% conformers have at least one gauche C-C bond in it.31 Clearly, the literature reports on the relative population of different conformers of n-hexane in the liquid phase are in conflict, which further complicate the analysis of its electronic spectra.

To obtain a comprehensive picture of the electronic structure of hexane and cyclohexane in liquid phase, two photon absorption (2PA) spectroscopy is used in our current study. With the help of *ab-initio* calculation, 2PA spectroscopy allows us to identify the nature of the electronic transitions in the energy range between 7-8.5 eV and to predict the extent of spectral shift and broadening upon solvation, especially the fate of the optically bright Rydberg transitions.

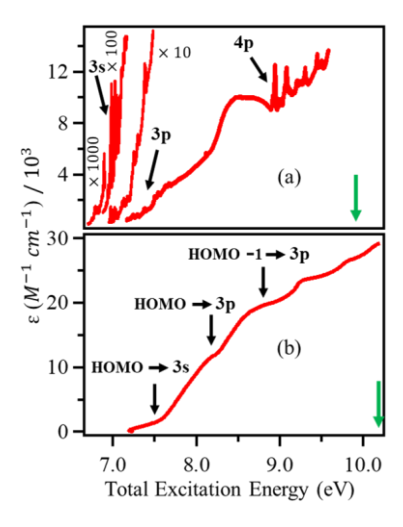


**Figure 1**: Experimental gas phase 1PA spectra of (a) cyclohexane and (b) n-hexane reproduced from  $Ref_{a}^{27}$  and  $Ref_{a}^{20}$ , respectively. The gas phase ionization energies are indicated by the green arrows. The important transitions, as per literature, are also marked in the Figure.

## II. Background: Gas phase 1PA spectra of cyclohexane and hexane

The gas phase 1PA spectra of cyclohexane (Figure 1a) shows two or more transitions in the region between 6.7 to 7.7 eV.<sup>22</sup> The lowest transition has a maximum at 7.13 eV and is associated with electron promotion from HOMO to Rydberg 3s orbital (LUMO).<sup>22</sup> Note that the HOMO and LUMO of cyclohexane in the chair conformation ( $D_{3d}$  point group) are of  $e_g$  and  $a_{1g}$  symmetries, respectively. According to Laporte selection rule,  $a_{1g} \leftarrow e_g$  electron promotion is one-photon forbidden, but is two-photon allowed. Excitation involving promotion from HOMO to 3s Rydberg orbital appears in the 1PA spectrum via vibronic coupling with an  $a_{2u}$  mode which has a ground state vibrational frequency of 522 cm<sup>-1</sup>.<sup>24</sup>, 32-33 The cluster of sharp peaks following the first transition are due to excitation to Rydberg 3p orbitals with a maximum at ~7.55 eV. The n=4 Rydberg transitions appear above 8.7 eV. The sharp peak ~ 9 eV can be assigned to the transition

Formatted: Left

Formatted: Font: 11 pt, Bold

Formatted: Font: 11 pt

Formatted: Left, Indent: First line: 0", Line spacing:

single

associated with promotion of electron to 4p Rydberg orbital. This 4p transition and other higher energy transitions show a vibronic progression of 1076 cm<sup>-1</sup>, which can be associated with a combination mode of C-C breathing vibration and C-C-C torsional mode with the frequency of 802 cm<sup>-1</sup> and 386 cm<sup>-1</sup> respectively.<sup>22</sup> The frequency of vibronic progression matches well with that observed in the photoelectron spectrum, 0.14 eV  $\approx$  1100 cm<sup>-1</sup>.<sup>22</sup> Other lower frequency progressions observed in the 1PA spectrum of cyclohexane show irregular spacing, which is a consequence of Jahn Teller splitting of the excited electronic states arising from the doubly degenerate  $\sigma$  bonding orbitals (HOMO) and the overtone/combination splitting due to anharmonicity of the potential energy surface.<sup>25</sup>

In contrast to the 1PA spectrum of cyclohexane in the gas phase, the hexane spectrum does not show any sharp features in the 7.0-10.0 eV region (Fig. 1(b)). Starting with the 9.3 eV band in ethane and applying independent system theory (bond additivity model) as mentioned above, Raymonda et al. Predicted the excitation energy in higher homologs of the alkane series. The calculated transition energies at 8.28 eV, 8.86 eV and 9.79 eV correlate well with the observed transitions at 8.37 eV, 8.99 eV and 9.55 eV that were extracted by fitting the gas phase 1PA spectra of n-hexane. They assigned these transitions to  $\sigma_{\text{C-C}} \rightarrow \sigma^*_{\text{C-C}}$  type, involving mainly C-C bonds of the molecule. A shoulder at a lower energy  $\sim 7.5$  eV was assigned to the charge transfer transition between adjacent C-C segments. Later, Au et al. An noticed the presence of this shoulder in the 1PA spectrum of ethane as well, which has only one C-C bond and consequently cannot have any charge transfer transition of this type. As a result, they argue that this transition involves HOMO $\rightarrow 3$ s electron promotion. An argue that this transition involves the HOMO $\rightarrow 3$ s electron promotion. Using the similarity of the transitions in the n-alkanes (n=3-8) and performing a term-value analysis, Au et al. Proposed that the 8.2 eV transition involves

combination of HOMO  $\rightarrow$  3p and HOMO-1  $\rightarrow$  3s electron promotion, and the 8.8 eV transition involves the HOMO-1 $\rightarrow$  3p promotion.

#### III. Methods

To better understand the electronic structures of alkanes and cycloalkanes in the liquid phase, in this work, we used two photon absorption (2PA) spectroscopy, which is guided by entirely different selection rules, and therefore, for a highly symmetric molecule like cyclohexane, may excite electronic states that are not symmetry allowed in conventional one photon absorption (1PA). Liquid cyclohexane was purchased from OmniSolv, 99.99%, spectrophotometric grade, lot # 40285; and liquid hexanes from Liquid cyclohexane was purchased from OmniSolv, 99.99%, spectrophotometric grade, lot # 40285; and liquid hexanes from EMD Chemicals Inc., 99.7%, lot # 46317. It is to be noted that liquid hexanes used in this study consist of different lower symmetry hexane isomers (2- and 3-methylpentanes) and methyl cyclopentane, with n-hexane present predominantly, ~61%. The continuous 2PA spectra in the energy range between 7-8.5 eV were measured by simultaneous absorption of a 266 nm (4.6 eV) pump photon and one UV-visible probe photon from the white-light continuum (1.8-3.9 eV). The pump and probe beams were overlapped spatially and temporally on the liquid sample delivered by a wire-guided gravity jet, <sup>35</sup> The 2PA spectra were recorded at both parallel and perpendicular polarization between the pump and probe photons. The details of the experimental set-up are described in a previous publication. <sup>18</sup>

To assign the character of transitions in gas phase cyclohexane and n-hexane and to predict the fate of these transitions upon solvation, *ab-initio* calculations were performed for the isolated molecules. The geometries were optimized at RI-MP2/cc-PVTZ level of theory. The excited electronic states were calculated for the optimized geometry using the equation-of-motion couple cluster (EOM-CC) method.<sup>36-37</sup> The transition energies, 1PA and 2PA cross sections were

calculated using the excitation energy method (EOM-EE-CCSD), with d-aug-cc-PVDZ basis set. The chair conformer of cyclohexane was used for the calculation. For n-hexane, two different conformers, all-trans (TTT) and trans-gauche-trans (TGT), were calculated. The rotationally averaged 2PA coefficient is calculated as:

$$\beta_{2PA} = \frac{F}{30} \sum_{a,b} S_{aa,bb} + \frac{G}{30} \sum_{a,b} S_{ab,ab} + \frac{H}{30} \sum_{a,b} S_{ab,ba}$$

Where S is transition strength matrix<sup>18</sup> and F, G, and H are integer constants that depend on the relative polarization of the two photons. For parallel linearly polarized light, F = G = H = 2; for perpendicular linearly polarized light, F = -1, G = 4, and H = -1.<sup>38</sup> The macroscopic 2PA cross section  $\sigma_{2PA}$  (in GM) was calculated from the orientationally averaged 2PA coefficient ( $\beta_{2PA}$ ) using the following equation:<sup>18,39</sup>

$$\sigma_{2PA} = \frac{2\pi^2 \alpha a_0^5 (\omega_1 + \omega_2)^2 \beta_{2PA}}{c * \Gamma * 10^{-50} * 27.2107}$$

where  $\alpha$  is the fine structure constant,  $a_0$  is the Bohr radius (in cm),  $\Gamma$  is lifetime broadening (0.1 eV),  $\omega_1$  and  $\omega_2$  are the energies of the two photons in eV ( $\omega_1 = 4.6$  eV in our experiments) and c is the speed of light (in cm/s). McClain and co-workers<sup>40-42</sup> have identified two important symmetry rules pertaining to  $\sigma_{2PA}$  values. (i) for transitions that lower the symmetry of the electronic wavefunction,  $\sum_{a,b} S_{aa,bb} = 0$ ; for those preserving electronic symmetry,  $\sum_{a,b} S_{aa,bb} > 0$ ; and (ii) for transitions preserving electronic wavefunction symmetry or in cases where the two photons have the same frequency (degenerate) regardless of symmetries involved in the transition,  $\sum_{a,b} S_{ab,ab} = \sum_{a,b} S_{ab,ba}$ . Using these rules, one can conclude that for any given point group, in degenerate experiments, the polarization ratio ( $\sigma_{||}/\sigma_{\perp}$ ) for non-totally symmetric transitions (assuming the ground state is totally symmetric) is always 4/3, but totally symmetric transitions

can have any value greater than 4/3. Moreover, in the case where one of the photons has energy very close to that of a molecular eigenstate (near resonance),  $\sum_{a,b} S_{aa,bb} = \sum_{a,b} S_{ab,ab}$ ; leading to  $\sigma_{||}/\sigma_{\perp}$  equal to ½ for a non-totally symmetric transition, whereas that for a totally symmetric transition is always 3.<sup>43</sup> Thus, under some special circumstances, the totally symmetric transition can be distinguished from the non-totally symmetric cases from symmetry considerations *alone*, without the need to perform extensive quantum mechanical calculations.

#### IV. Results

All calculated transition energies and 1PA and 2PA cross sections are tabulated in Table S1-S3 of the Supporting Information and are shown as the stick spectra in Figure 2. Important transitions in 1PA and 2PA for cyclohexane and the TTT conformer of n-hexane are tabulated in Tables 1-2.

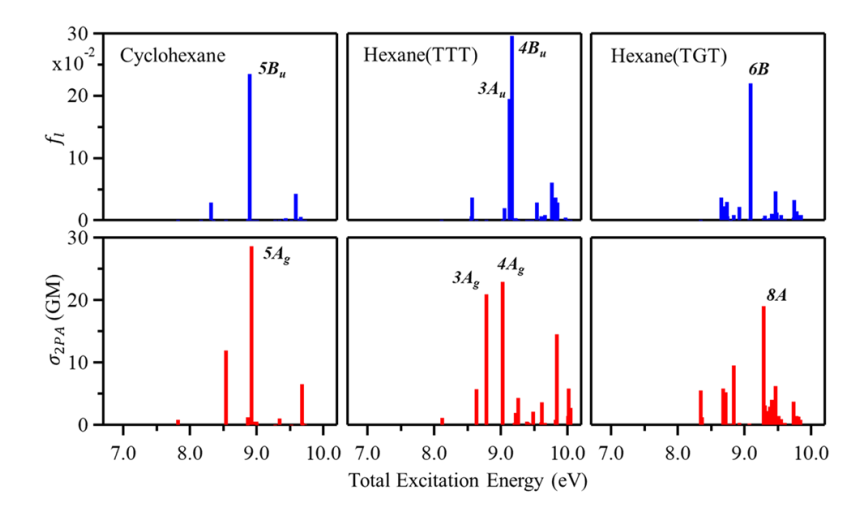


**Figure 2:** Calculated 1PA and 2PA transitions for cyclohexane, hexane-all-trans (TTT) and hexane-transgauche-trans (TGT) at EOM-CCSD/d-aug-cc-PVDZ level of theory. 2PA cross sections are calculated using 4.6 eV pump energy. For the strongest 1PA and 2PA transitions, the sticks are labeled with the upper state character.

Formatted: Font: 11 pt, Bold

Formatted: Font: 11 pt

The point group symmetries of the chair conformation of cyclohexane and the TTT conformer of n-hexane are  $D_{3d}$  and  $C_{2h}$  respectively. For cyclohexane, the excited state symmetry labels reported in Table 1 correspond to one of the Abelian subgroups  $(C_{2h})$  of  $D_{3d}$ . To allow ready correspondence with the spectroscopic existing literature on cyclohexane that follows the  $D_{3d}$  point group notation, we show the mapping between the spectroscopic term labels of  $D_{3d}$  and  $C_{2h}$  groups in Table S4 of the Supporting Information. 44 Because of the presence of inversion symmetry in cyclohexane, 1PA active transitions are inactive in 2PA and vice versa. The symmetry of the ground electronic state is  $1A_g$ , hence transitions to electronic states of 'gerade' and 'ungerade' symmetries are expected to be 2PA and 1PA allowed, respectively. For example, in cyclohexane, the  $5A_g \leftarrow 1A_g$  transition is most intense in 2PA, whereas the  $5B_u \leftarrow 1A_g$  transition is strongest in 1PA. The TGT conformer of n-hexane, on the other hand, has a C<sub>2</sub> point group symmetry. The lack of inversion symmetry in this point group allows all the excited electronic states of A and B character to be both 1PA and 2PA active (Table S3). Although these two alkane molecules only have six C atoms, the density of states is already very high, as evident from the number of calculated electronic states within ~9.5 eV (Table S1-S3, Figure 2). Due to such high electronic density of states, several transitions with different symmetries (e.g.,  $5A_g \leftarrow 1A_g$  and  $5B_u \leftarrow 1A_g$ ) have almost the same energy (Figure 2).

Natural transition orbital (NTO) analysis is performed to characterize the excited states and to visualize the nature of the participating orbitals in a particular transition. To readily identify a transition as Rydberg transition or valence transition or mixed, the relative change in the size of the wavefunction following an excitation ( $\Delta < R^2 >$ , Å<sup>2</sup>) is calculated. For transitions to valence states,  $\Delta < R^2 >$  should be small, but a large value is expected for transitions to Rydberg states.

Taking trans-stilbene as an example, the lowest energy excitation has a pure valence character with a  $\Delta < R^2 >$  value of 0.1 Å<sup>2</sup>.<sup>45</sup> On the other hand, we see that the calculated  $\Delta < R^2 >$  values for all the strong 1PA and 2PA active transitions in cyclohexane (Table 1) and both conformers of n-hexane (Table 2 & S3), are much larger; it is clear that all these transitions are of predominantly Rydberg character for these molecules at least when isolated in vacuum.

Table 1. Selected calculated electronic transition energies ( $E_{ex}$ ) and their properties for cyclohexane (EOM-CCSD/d-aug-cc-PVDZ). Two-photon strengths assume a 4.6 eV fixed photon energy. Most intense transitions in bold.

State	$E_{ex}$ (eV)	$f_{IPA}$	$\beta_{2PA}$	$\sigma_{2PA}$ (GM)	2PA	$\Delta < R^2 >$	Transition
		$(\times 10^{-3})$	(atomic		polarization	$(\mathring{A}^2)$	assignment
			units)		ratio (ρ)	, ,	
$2A_g$	7.83		18.6	0.8	1.3	14.3	HOMO→R3s
$lB_g$	7.83		18.7	0.8	1.3	14.3	HOMO→R3s
$3A_g$	8.54		221	11.9	3.3	13.9	HOMO-1→R3s
$4A_g$	8.87		21.3	1.2	1.3	25.9	HOMO→R3d
$2B_g$	8.87		21.3	1.2	1.3	25.9	HOMO→R3d
$5A_g$	8.92		489	28.6	22.6	28.0	HOMO→R3d
$2A_u$	8.32	28				19.5	HOMO→R3p
$3B_u$	8.32	28				19.5	HOMO→R3p
$5B_u$	8.89	235				14.4	HOMO-1→R3p

Table 2. Selected calculated electronic transitions energies ( $E_{ex}$ ) and their properties for hexane-TTT (EOM-CCSD/d-aug-cc-PVDZ). Two-photon strengths assume a 4.6 eV fixed photon energy. Most intense transitions in bold.

State	$E_{ex}$ (eV)	$f_{IPA}$ (×	$\beta_{2PA}$	$\sigma_{2PA}$	2PA	$\Delta < R^2$	Transition assignment
		$10^{-3}$ )	(atomic	(GM)	Polarization	>, (Å <sup>2</sup> )	
			unit)		ratio (ρ)		
$2A_g$	8.12		23.0	1.1	2.0	10.4	HOMO→R3s
$lB_g$	8.64		104	5.7	1.3	10.0	HOMO-1→R3s
$3A_g$	8.78		369	20.9	21.3	11.7	HOMO-2→R3s
$4A_g$	9.03		383	22.9	5.5	27.9	HOMO→R3d + HOMO-1→R3d
$2B_u$	8.57	36.9				17.5	HOMO→R3p
$3B_u$	9.05	19.6				15.4	HOMO-2→R3p
3A <sub>u</sub>	9.13	195				14.1	HOMO-1→R3p + HOMO-2→R3p
4B <sub>u</sub>	9.17	296				15.1	HOMO-1→R3p + HOMO-2→R3p

Turning to the experimental spectra now, we will first discuss the 1PA spectra of hexane and cyclohexane in the liquid phase. Liquid alkanes and cycloalkanes generally have very strong absorption in the VUV region, making it difficult to measure the transmission spectra due to rapid attenuation of the incident photon beam. A light source with high photon-flux, a short optical pathlength along with highly sensitive photon detection are required to measure the transmission spectra of these molecular liquids. The most difficult task is to make very thin liquid films that can be kept under constant vapor pressure to avoid evaporation and maintain a constant thickness during data acquisition. Using a synchrotron beam source and an optical pathlength of  $1 \pm 0.5 \,\mu m$ , Jung and Gress<sup>46</sup> measured the transmission 1PA spectrum of liquid cyclohexane, as reproduced in Figure 3(a). Costner et. al.<sup>47</sup> measured the transmission spectra of liquid alkanes in the farultraviolet (FUV) region. The liquid alkane spectra are relatively simple with a single broad transition in the FUV region. But, due to very strong absorbance of this band, they could not capture where this transition actually comes to a peak using their transmission set-up (Figure 3b, inset). To overcome this problem, Ozaki and coworkers<sup>48</sup> introduced attenuated total reflection (ATR) technique in the FUV region, and measured a spectrum of liquid n-hexane up to 8.6 eV (Figure 3b), allowing one to clearly identify the peak of this broad transition. However, one should keep in mind that the ATR-FUV spectrum is not identical with the corresponding transmission spectrum. In the transmission experiment, the pathlength is defined by the thickness of the sample and is therefore constant across the spectrum. On the other hand, in the ATR experiment, the depth to which the sample is penetrated by the light beam is a function of wavelength of light, and wavelength-dependent refractive indices of the ATR crystal and the sample. The refractive index of the sample changes sharply around absorption bands and thus the wavelength dependent penetration depth is further modified distorting the relative peak intensities, as well as a slight

change in the peak positions. Moreover, the ATR spectra of liquid alkanes by Ozaki and coworkers are reported without any ATR correction or Kramers-Kronig transformation, as the cut-off region at ~8.5 eV is so flat that extrapolation to zero intensity becomes difficult.<sup>49</sup> Nevertheless, the reported ATR spectrum gives us an approximate idea of where the transition in liquid n-hexane peaks in the FUV region, that would otherwise difficult to measure using conventional transmission experiments.

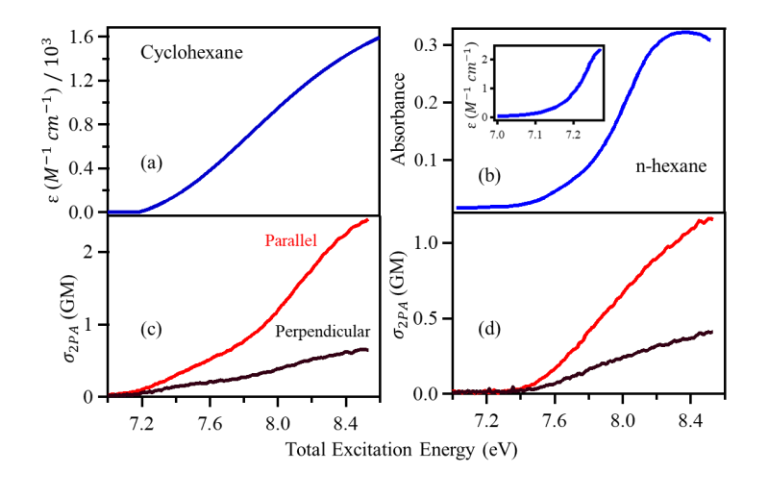


Figure 3; (a) Liquid 1PA spectrum of cyclohexane, by transmission method, digitized from Ref<sup>16</sup> and converted to ε using the A = εcl equation, where the path length l is 1 μm. (b) Liquid 1PA spectrum of n-hexane, by ATR-FUV method; digitized from Ref<sup>18</sup> Here the y-axis has not been converted to ε, as light penetration inside the liquid phase in an ATR-FUV experiment is wavelength dependent. A VUV transmission spectrum (in ε unit) of liquid hexane is shown in the inset, and digitized from Ref<sup>17</sup> Liquid 2PA spectra of (c) cyclohexane and (d) n-hexane (this work). The 2PA cross sections are measured with both parallel and perpendicular polarizations of the pump and probe beams. The pump photon energy is 4.6 eV for our experiment.

In contrast to gas-phase 1PA cross-section (Figure 1), absolute 2PA cross section ( $\sigma_{2PA}$ ) of cyclohexane in liquid phase (Figure 3c) is twice as large as compared to n-hexane (Figure 3d), pointing to the fact that 1PA and 2PA spectra are dominated by different sets of excitations in these

Formatted: Font: 11 pt, Bold	
Formatted: Font: 11 pt	

molecules. The 2PA spectra are reported for both parallel and perpendicular polarization of the pump and probe photons, where the energy of the pump pulse is 4.6 eV. For both the molecules, parallel polarization of the two photons give rise to a higher cross section as compared to that of perpendicular polarization. It is also apparent from these spectra that cyclohexane has a lower energy 1PA and 2PA threshold as compared to n-hexane. This is consistent with our *ab initio* calculation where the lowest excited state of cyclohexane appears at 7.8 eV and the first strong 1P and 2P transitions are at 8.3 and 8.5 eV respectively, whereas in hexane-TTT the lowest excited state is at 8.1 eV, with the first strong 1P and 2P transitions are at 8.6 and 8.9 eV, respectively. For hexane-TGT conformer, the first strong transitions are also higher but now inverted at 8.7 and 8.4 eV.

Another interesting difference is observed in the polarization ratio plots of these molecules, as shown in Figure 4. In case of cyclohexane, the polarization ratio increases almost linearly from  $\sim$ 1.7 at 7.0 eV to  $\sim$ 4 at 8.5 eV. A polarization ratio > 4/3 in the entire spectral region suggests that transitions in cyclohexane are dominated by totally-symmetric type excitations, particularly the brightest transitions that have very high polarization ratio (see Table 1).<sup>42</sup> The decrease in polarization ratio in the lower energy region is presumably a consequence of the contributions from the lower polarization ratio  $2A_g \leftarrow 1A_g$  and  $1B_g \leftarrow 1A_g$  transitions, which involve promotion of electrons from doubly degenerate HOMO to the 3s Rydberg orbital ( $e_g \rightarrow 3s$ ) of cyclohexane (shown in Figure 5). The polarization ratio of hexane, on the other hand, rises instead (and more quickly) from a value near  $\sim$ 1.0 reaching only  $\sim$ 2.5 in the 7-8 eV region; it maintains an almost constant value in the higher energy region. It is worth pointing out that, in case of both liquid cyclohexane and hexanes, trace amounts of 2-photon pump photoionization products (e.g.,

solvated electrons) could also contribute (as a transient absorption signal) to the low polarization ratio in the lower energy part of the spectra.<sup>50-52</sup>

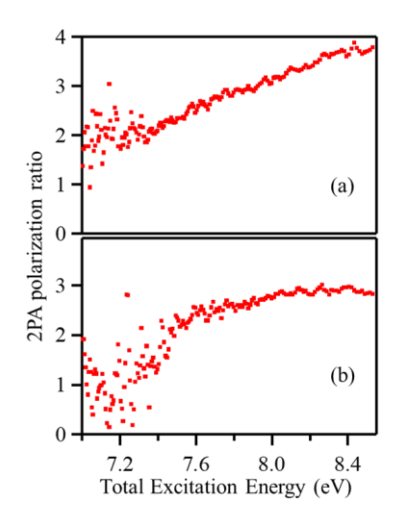


**Figure 4:** 2PA polarization ratio plot of (a) cyclohexane and (b) n-hexane (this work). The pump photon energy used in our experiment is 4.6 eV.

### V. Analysis

V.A. Liquid cyclohexane.

We will first compare the assigned gas-phase one-photon transitions in cyclohexane with the excited energy levels obtained by our *ab initio* calculation of a single cyclohexane molecule. A transition associated with electron promotion from HOMO to Rydberg 3s orbital appears at  $\sim$ 7.13 eV in the gas phase spectrum of cyclohexane. This transition is electronically forbidden but only vibronically allowed in 1PA. Our *ab initio* calculation for cyclohexane indeed predicts that the first two transitions at 7.83 eV ( $2A_g \leftarrow 1A_g$  and  $1B_g \leftarrow 1A_g$ ) consistent with this assignment; the transition degeneracy comes from the doubly degenerate HOMO ( $e_g$  symmetry). According to

Formatted: Font: 11 pt, Bold

Formatted: Font: 11 pt

Raymonda et al.,  $^{22}$  the first symmetry-allowed Rydberg transition associated with HOMO $\rightarrow$ 3p electron promotion appears at 7.77 eV in the gas phase spectrum of cyclohexane. The energy of this transition is predicted to be at 8.3 eV according to our calculation. The error in calculating excited state energies by EOM-EE-CCSD method is typically 0.1-0.3 eV for excitations associated with a single electron promotion.  $^{53-55}$  Calculated transition energies which have substantial double excitation character, as in case of cyclohexane due to the degeneracy in its bonding molecular orbitals, may lead to an error up to  $\sim$  1 eV.  $^{56}$ 

Natural transition orbitals (NTO) analysis reveals that 1PA and 2PA allowed transitions are dominated by electron promotion to 'p' and 'd' type Rydberg orbitals, respectively, except for the first three 2PA allowed transitions: the degenerate transitions  $2A_g \leftarrow 1A_g$  and  $1B_g \leftarrow 1A_g$  just discussed and the  $3A_g \leftarrow 1A_g$  transition, which has reasonable 2P cross section and is due to HOMO-1  $\rightarrow$  3s electron promotion. The NTO plots corresponding to the strong transitions in cyclohexane 1PA and 2PA are shown in Figure 5.

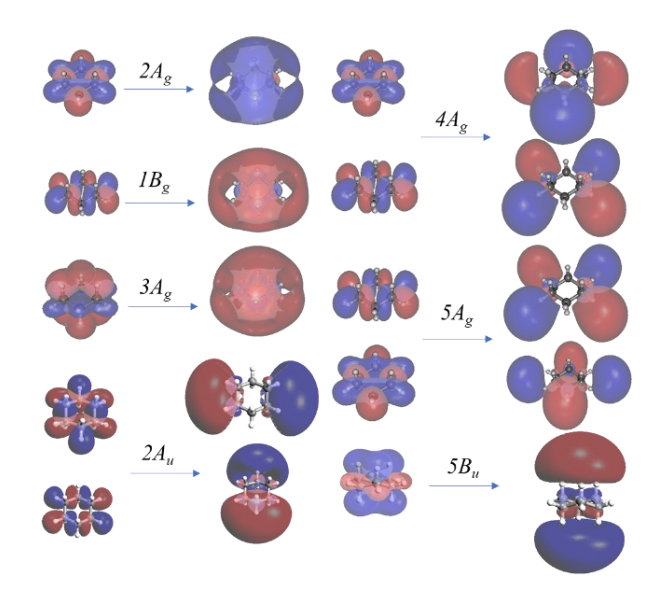


Figure 5: NTO plots corresponding to the strong transitions of cyclohexane in 1PA and 2PA

Jung et. al<sup>46</sup> reported the 1PA spectrum of liquid cyclohexane (Figure 3a; the full spectrum is in Figure S1 of the Supporting Information) in the range between 6-11 eV. The absorption threshold was estimated to be  $7.0 \pm 0.1$  eV. Gaussian fitting of the liquid 1PA spectra revealed a first peak at ~7.8 eV with the FWHM of ~0.8 eV and a second peak ~8.7 eV with ~1.4 eV FWHM. Comparing with the gas phase spectra of cyclohexane, they assigned the first and second peaks in the liquid phase spectrum to the transitions involving 3p and 3d Rydberg orbitals. They did not however assign any transition to 3s Rydberg states in the liquid phase based on their spectrum; such transitions (like those to the 3d) are strictly parity forbidden. Jung et al.'s analysis of the liquid 1PA spectrum of cyclohexane predicts a larger Gaussian width for transitions at higher energy, which interestingly matches our observation for liquid water and alcohols.

The approach adopted by Jung et. al<sup>46</sup> to fit the liquid 1PA spectra with multiple Gaussians and use these Gaussian peaks to assign transitions in liquid phase is somewhat arbitrary. In contrast, we simulate the liquid 1PA and 2PA spectra as well as the polarization ratio spectrum using results obtained for the appropriate isolated molecule from *in vacuuo* quantum chemistry calculation. We incorporate all excited state transitions that have impact on the experimental energy range, along with their respective transition strengths.

Prior to performing the spectral simulations, we perform a correction to address the known deficiency in the calculated gas-phase transition energies. We red-shift all transitions by ~0.6 eV in order to approximately match with the experimental gas phase transitions described above. The common sets of parameters that simultaneously reproduce all the spectra are reported here: the transitions up to ~8 eV are broadened by ~0.7 eV, and above that, a FWHM of ~1.1 eV is used. Excitations involving '3s' type upper Rydberg orbitals  $(2A_g \leftarrow 1A_g, 1B_g \leftarrow 1A_g)$  and  $3A_g \leftarrow 1A_g$ 

Formatted: Font: 11 pt, Bold

Formatted: Font: 11 pt

require blue-shifting by 0.55 eV to account for the effect of the solvent environment; all other transitions experience negligible solvatochromic shift. The oscillator strengths for each transition are used directly from the calculation; a single overall scaling is used to best agree with experimental extinction coefficient. We acknowledge the entirely empirical gas-to-liquid phase energy shifting employed; an accurate first principles description of the electronic structure of a repeating molecular liquid with delocalized excited states is still a frontier research problem for theory.

As shown in Table 1 and Figure 2, the 1PA transitions in cyclohexane involve the excited states of 'ungerade' symmetry and thereby, are comprised of a completely different sets of excitations than the 2PA spectrum. Despite the mutually exclusive transitions in 1PA and 2PA, the liquid 1PA spectrum can be reproduced by allowing similar shifts and broadening to the 1PA active transitions as done for the 2PA active transitions during 2PA simulation. The simulated plots are shown in Figure 6.

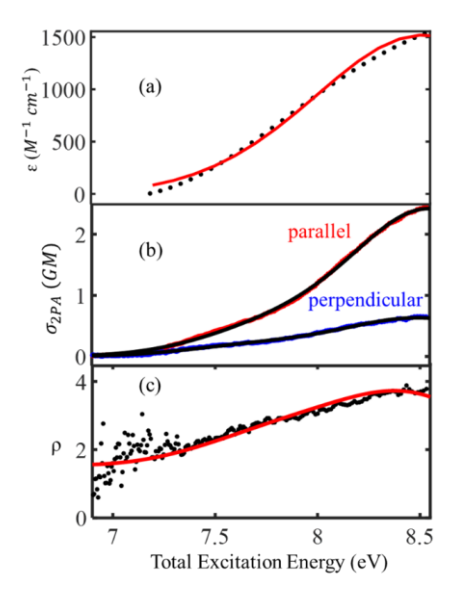


Figure 6: (a) Simulation of 1PA spectrum of liquid cyclohexane. The raw data (black dots) is digitized from Ref. and the red line stands for the simulated plot. Simulation of (b) 2PA spectra of cyclohexane for parallel (red) and perpendicular (blue) polarization combinations, and (c) the polarization ratio. The calculated transition energies are all red-shifted by  $\sim 0.6$  eV to compensate for the systematic error of the EOM-CCSD calculation. The transitions up to  $\sim 8$  eV are broadened by  $\sim 0.7$  eV, and above that, a FWHM of  $\sim 1.1$  eV is used. Excitations involving '3s' type upper Rydberg orbitals  $(2A_g \leftarrow 1A_g, 1B_g \leftarrow 1A_g \text{ and } 3A_g \leftarrow 1A_g)$  only are given an additional blue-shift of  $\sim 0.55$  eV; all the other transitions do not require further shifting.

The  $\sim$ 0.55 eV gas to liquid blueshift of the Rydberg transitions involving the 3s orbital in cyclohexane is similar to our previous findings for electronic spectra of water<sup>43</sup> and alcohols. <sup>18</sup> The transition in cyclohexane involving promoting the HOMO  $\rightarrow$  3s is parity forbidden and therefore extremely weak in 1PA and thus Jung et al. <sup>46</sup> could not assign this transition when fitting the liquid 1PA spectrum. However, in 2PA, this transition is now symmetry allowed and appears as a clear shoulder at  $\sim$ 7.6 eV in the 2PA spectra. To accurately reproduce this shoulder, a  $\sim$ 0.55

Formatted: Font: 11 pt, Bold

Formatted: Font: 11 pt

Formatted: Font: 11 pt

Formatted: Font: 11 pt

eV blue shift for the lowest calculated transition (appearing at  $\sim$ 7.1 eV in gas phase spectrum) is necessary.

We have also previously seen that the polarization ratio spectrum is an extremely sensitive tool in 2PA spectroscopy. Any change in the polarization ratio reflects the contribution from multiple excited states. The polarization ratio provides a discerning constraint during the simulation of the 1PA and 2PA spectra. Therefore, the good match between the experimental and the simulated polarization ratio for cyclohexane, using a common set of parameters in simulating the 1PA and 2PA spectra, is encouraging. We re-emphasize that, except for shifting transitions ending in the 3s Rydberg state, the calculated gas phase transition energies (after correction) and relative oscillator strengths are used unaltered in our simulation of the liquid phase spectra. Our approach thus emphasizes the usefulness of the isolated-molecule electronic structure calculation as a reasonable starting point to investigate the fate of electronic transitions in the condensed phase, particularly for molecules with no low lying valence excitations.<sup>57</sup>

#### V.B. Liquid Hexane.

Simulation of liquid hexanes spectrum is more challenging as there are several conformations of the n-hexane molecule present at room temperature and no consensus on the relative populations of these conformers in the literature reports.<sup>30-31</sup> It is also noteworthy that the sample used in our experiment was ~61-2% pure in n-hexane, with impurity due to branched (2-and 3-methylpentanes) and cyclic alkanes (methyl cyclopentane). Despite this, it will be interesting to observe how the electronic structure of six-carbon lower symmetry acyclic conformers develop compared to their highly symmetric cyclic counterpart, cyclohexane. We have performed EOM-CCSD calculations to obtain the excited state energies and 1PA and 2PA cross sections for two

different representative conformers of n-hexane, all-trans (TTT) and trans-gauche-trans (TGT), as shown in Figure 2. The calculated transition energies differ by ~0.1-0.3 eV between these two conformers (contrast Table S2 & S3). The all-trans conformer (TTT) has inversion symmetry resulting in the 1PA active transitions to be 2PA inactive and vice versa. The lack of inversion symmetry in the TGT conformer allows all the excited electronic states to be both 1PA and 2PA active. The different point group symmetries of these two conformers therefore directly influence the transition strengths as evident from our calculated 1PA and 2PA cross sections.

As discussed above, Au et al.<sup>34</sup> assigned the 8.2 eV band (Figure 1b) of an isolated hexane molecule to the transition associated with combination of HOMO → 3p and HOMO-1 → 3s electron promotion and the 8.8 eV band to a transition involving HOMO-1→ 3p electron promotion. Our theoretical calculation also predicts similar transitions (as evident from the NTO analysis, Figure 7) but are typically overestimated by 0.3-0.4 eV for both conformers, similar to the case of cyclohexane. To gain a crude approximation about the shifts and broadening of the excited states upon solvation, we first start with simulating the liquid phase 1PA spectra of n-hexane using the theoretically calculated results for the isolated molecule. The experimental spectra can be fit based on the gas phase calculation with transitions red-shifted by 0.78 eV and 0.65 eV for the TTT and the TGT conformers, with a broadening of 0.76 eV and 0.66 eV, respectively. Such red-shift of the calculated transitions required to simulate the liquid 1PA spectra include both the solvatochromic shift and the systematic error of the EOM-CCSD approach due to its intrinsic limitation of not including higher order excitations (triples and above).<sup>45, 53-55, 58</sup> The simulated plots are shown in Figure S2 of the Supporting Information.

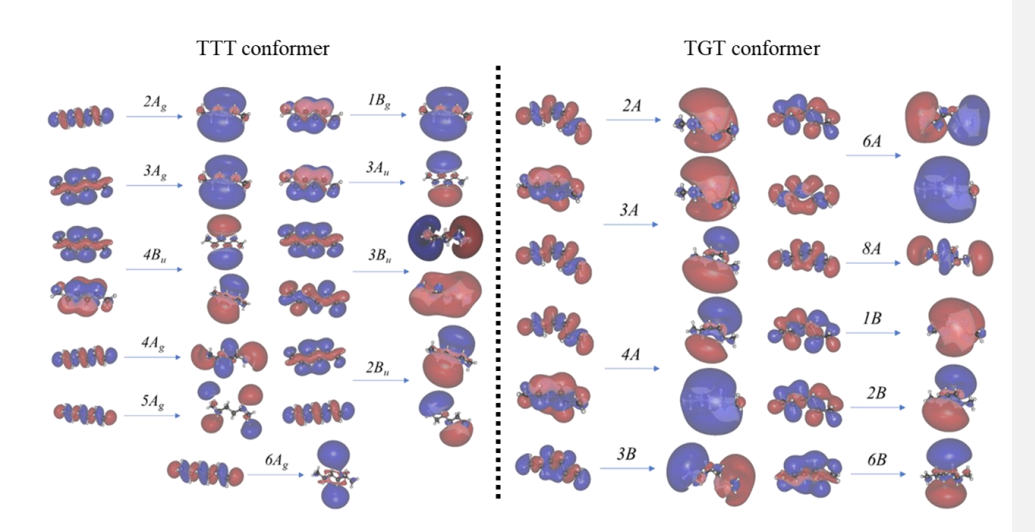


Figure 7: NTO plots corresponding to the strong transitions of the TTT and the TGT conformers of n-hexane in 1PA and 2PA.

As discussed above, the experimental liquid 1PA spectrum of n-hexane (figure 3b) shown here is measured using an ATR-FUV spectrometer,  $^{48}$  which is known to cause a shift in the peak position as well as the peak intensity. As a result, simulation of the liquid 1PA spectra of n-hexane gives us only a rough estimate of shifting and broadening of electronic states upon solvation. To be more quantitative, we simulate our measured 2PA spectra using the theoretically calculated transition energies and the 2PA cross sections as tabulated in Table S2-S3. The general parameters that simultaneously reproduce the 2PA spectra for both parallel and perpendicular polarization combinations, along with the polarization ratio are as follows. First, all calculated transitions are red-shifted by 0.35 eV (for TTT) and 0.4 eV (for TGT) to account for the intrinsic computational error of the EOM-CCSD method. Then, an additional solvatochromic red-shift of  $\sim$ 0.15-0.2 eV is given to each energy level except for the transition associated with HOMO $\rightarrow$ 3s electron promotion ( $2A_g \leftarrow 1A_g$  in TTT and  $2A \leftarrow 1A$  in TGT conformer), which is instead blue-shifted by  $\sim$ 0.18 eV. As

Formatted: Font: 11 pt, Bold

Formatted: Font: 11 pt

we allow the bandwidth of each transition float freely during our simulation, they adopt a value of 0.9 eV and 0.65 eV for the TTT and the TGT conformers, respectively. The simulated plots for are shown in Figure 8. Although both simulations capture the experimental trend of increase in 2PA cross section with increasing energy, the experimental spectrum is reproduced more closely using the electronic structure of the TGT conformer, reflecting the presence of considerable amount of lower symmetry isomers in the liquid phase. None of these conformers alone can fully reproduce the experimental polarization ratio. As shown by Costner et al., 47 cyclic impurities like methylcyclopentane are expected to have a slightly lower-energy absorption onset as compared to that of linear-chain hexanes. The concentration of these cyclic isomers is relatively low in liquid hexanes; therefore, their contribution towards the 2PA spectra would only be apparent in the red tail of the absorption band, where no other hexane isomer absorbs. As a result, such impurities may have an out-sized impact in the region of the absorption onset of liquid hexanes, resulting to an abrupt drop in polarization ratio below ~7.5. This reinforces the idea that the polarization ratio is an extremely sensitive quantity in capturing the character of the electronic transitions in the 2PA spectra. Our analysis, using two representative isomers of n-hexane, thus casts light on the general solvatochromic shifts and broadening of lower symmetry acyclic conformers of a hexane molecule and enables us to compare these results with its cyclic counterpart. Below we discuss the results of our analysis for these two representative alkanes.

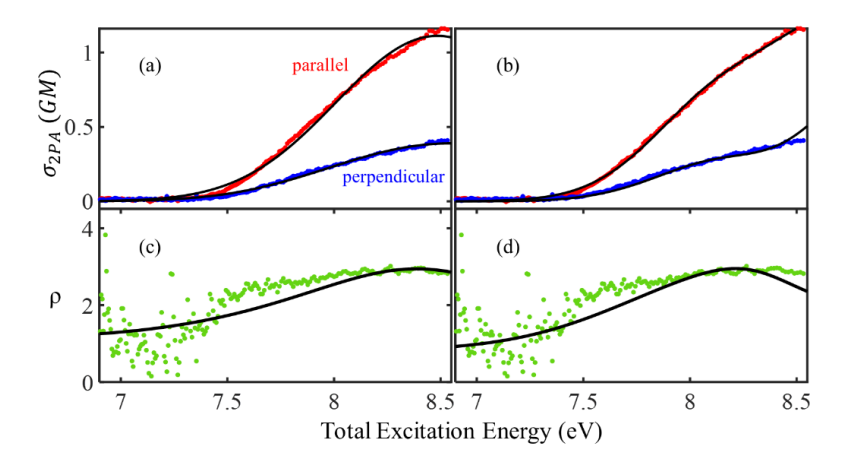


**Figure 8**: Simulation of the parallel and perpendicular 2PA spectra of n-hexane using theoretical calculated results for (a) TTT and (b) TGT conformers. The simulation of the polarization ratio is obtained using theoretical calculated results for (c) TTT and (d) TGT conformers. The green dots and the black lines represent the raw data and the simulated plots respectively. The parameters of these simulations are mentioned in the text.

#### VI. Discussion

The first absorption band of cyclohexane in liquid phase appears at a lower energy compared to that of liquid n-hexane, which, interestingly, coincides well with the lower ionization energy of cyclohexane vs n-hexane in the gas phase (9.9 eV vs. 10.2 eV).<sup>47</sup> Typically, the smaller ionization energies of cycloalkanes as compared to their linear alkane homologues are attributed to the destabilization of the HOMO in the former due to ring strain. However, cyclohexane has negligible ring strain because of the puckering of its backbone. Instead, Costner et al.<sup>47</sup> showed that the absorption spectra of linear alkanes and cycloalkanes shift to the lower energy with the increase in the number of carbon atoms in the alkyl or cycloalkyl chain. By performing term value analysis, they concluded that the addition of carbon atoms destabilizes the HOMO while the energy of Rydberg LUMO orbital is not affected, resulting in a redshift of the absorption spectra as well

Formatted: Font: 11 pt, Bold

Formatted: Font: 11 pt

as the ionization potential. Using this argument, cyclohexane contains an extra C-C bond compared to n-hexane, causing destabilization of its HOMO and thereby results to a redshift of the first absorption band and ionization potential. This is consistent with our gas phase *ab initio* calculation, where the first absorption band of cyclohexane is predicted to be ~0.3 eV lower in energy than that of the all-trans (TTT) conformer of n-hexane.

As in 1PA, liquid cyclohexane has a lower 2PA threshold ( $\sim$ 7.3 eV) compared to that of n-hexane ( $\sim$ 7.6 eV). A small shoulder, corresponding to the lowest energy transition associated with HOMO  $\rightarrow$  Rydberg 3s type electron promotion, is observed at  $\sim$ 7.6 eV in cyclohexane 2PA spectrum, bringing the 2PA threshold down. The 2PA threshold of both alkanes are higher than that of alcohols ( $\sim$ 7.2 eV), but lower than that of water ( $\sim$ 8.2 eV). This can be important in choice of solvent for femtosecond pump probe spectroscopy where ultraviolet pump pulses are being used to study the solute's behavior, but the signal can be dominated by two-photon induced process from the large excess of solvent.

For cyclohexane, the transitions that involve the promotion of electrons to the Rydberg 3s orbital are  $2A_g \leftarrow 1A_g$  and  $1B_g \leftarrow 1A_g$  (degenerate, HOMO  $\rightarrow$  3s) and  $3A_g \leftarrow 1A_g$  (HOMO-1  $\rightarrow$  3s). From our analysis, these transitions experience a gas to liquid blue-shift of ~0.55 eV. In comparison, the  $4a_1 \leftarrow 1b_1$  and the  $1A'' \leftarrow 1A'$  transitions, respectively in water and alcohols, are also associated with  $2p_z \rightarrow 3s$  electron promotion and are similarly blue-shifted by ~0.9 eV upon solvation. It is reasonable to assign these blueshifts as a result of the Pauli repulsion experienced by the upper orbital due to the confinement by the surrounding solvent molecules. In case of water and alcohols, the orbitals that participate in the  $2p_z \rightarrow 3s$  type electron promotion are mainly centered on the oxygen atom where the hydrogen bonding takes place. As a result, promotion of electron from an out of plane  $2p_z$  orbital to a spherically distributed 3s orbital

increases electron density in the direction of the hydrogen bonding<sup>18</sup> and thereby is subject to greater Pauli repulsion resulting to a larger blueshift.

There are three factors that can be expected to determine the energetic shifting of a transition in going from gas to liquid phase: 1. Pauli repulsion in the excited electron experienced by the diffuse promoted electron with the surrounding solvent molecules, which destabilizes the excited state; 2. Stabilization of the excited state cationic core via instantaneous polarization of the surrounding solvent molecules, causing a red-shift relative to the gas phase transitions. 12 This can be assessed from the change in overall ionization potential in the two phases 3. Possible delocalization of the promoted electron over orbitals of multiple alkane molecules. Along with above factors, the y-Yan der Waals interaction particularly with diffuse Rydberg electron clouds between diffuse electron clouds may also play an important role in energetic shifting of the excited states upon solvation. Using a solvation model with state-specific polarizability (SMSSP), Marenich et al.<sup>59</sup> showed that the dispersion contribution depends on the spherically averaged molecular polarizability of the solute molecule (either in its ground or excited electronic state), and the refractive index of the solvent. The solvatochromic shifts due to dispersion are usually red, 60 as polarizability of the excited-states ( $\alpha_{ES}$ ) are generally larger than that of ground stats  $(\alpha_{GS})$ ; however, the extent of shift will be dependent on the polarizability of the excited orbitals (s, p or d type). A blueshift of ~0.55 eV for the transition associated with HOMO/HOMO-1  $\rightarrow$  3s electron promotion in cyclohexane suggests that Pauli repulsion plays the dominant role for the 3s orbital. Similar character transitions in n-hexane  $(2A_g \leftarrow lA_g \text{ in TTT and } 2A \leftarrow lA \text{ in TGT})$  also experience a solvatochromic blue-shift, but of smaller magnitude, ~0.18 eV. This difference may be traceable to difference in solvent packing. The density of all hexane isomers are approximately equal, ranging between 0.645-0.657 g/cm<sup>3</sup> at room temperature.<sup>28</sup> The density of liquid cyclohexane is 0.774 g/cm<sup>3</sup>, however, a value ~20% higher than that of liquid hexane.<sup>61</sup> In addition, the calculated  $\Delta < R^2 >$  value (isolated-molecule) for transitions to 3s Rydberg orbitals in cyclohexane (14.3 Å<sup>2</sup>, Table1) is higher than that of the TTT (10.4 Å<sup>2</sup>, Table2) and TGT (12.2 Å<sup>2</sup>, Table S3) conformers of n-hexane. This points to the fact that the relative change in the size of the wavefunction following promotion of electron to 3s Rydberg orbital is greater in case of cyclohexane. The larger spatial size of the 3s Rydberg orbital of a central cyclohexane molecule, coupled with its higher density in the molecular liquid, results in it experiencing greater Pauli repulsion from the neighboring solvent molecules, leading to a larger blue-shift as compared to that for straight chain hexanes. Moreover, unlike cyclohexane, the '3s' orbital of n-hexane are not of pure Rydberg type; instead, it is mixed with valence antibonding  $\sigma_{C-H}^*$ , as shown in Figure 7. Such valence-Rydberg mixing distorts the spherical symmetry of the Rydberg 3s orbital, resulting in a dumbbell-shaped electronic distribution, which, because of its smaller surface area, potentially experiences lesser Pauli repulsion from surrounding molecules in the solvation shell compared to that in cyclohexane.

From our analysis, the remaining transitions in cyclohexane can be fit assuming zero solvatochromic shift, whereas for n-hexane, the transitions are red-shifted by ~0.15-0.2 eV. For transitions involving higher level Rydberg orbitals, the excited electrons are more spread out in space, leaving the cationic core more poorly screened and therefore allowing greater polarization stabilization for the excited electronic state. Consequently, we might infer that for the higher energy Rydberg transitions in cyclohexane at least, the Pauli repulsion and the cationic stabilization nearly cancel each other. In case of liquid n-hexane, the higher Rydberg excitations experience lesser Pauli repulsion (due to smaller liquid density than that of cyclohexane) and the polarization stabilization of the cationic core is even more facile due to higher polarizability of n-

hexane (11.94 Å<sup>3</sup>) as compared to that of cyclohexane (11.04 Å<sup>3</sup>).<sup>62</sup> These two factors combined result in a general redshift of the higher energy Rydberg transitions in going from the gas to liquid phase of n-hexane.

In the case of cyclohexane, the most intense bands in 1PA and 2PA spectra in the studied energy range are dominated by the transitions involving promotion of electrons to the Rydberg 'p' and 'd' type orbitals, respectively; for example, the  $5A_g \leftarrow 1A_g$  transition (electron promotion to Rydberg 3d) is the most intense in 2PA, whereas the  $5B_u \leftarrow 1A_g$  transition (electron promotion to Rydberg 3p) is strongest in 1PA. The  $5A_g \leftarrow 1A_g$  transition also shows the highest polarization ratio. The experimental 2PA spectra is mainly dominated by this transition as evident from the steady increase in the 2PA cross section and an almost linear increase in the polarization ratio in our experimental spectral range. The decrease in polarization ratio in the lower energy region is likely a consequence of contributions from the  $2A_g \leftarrow 1A_g$  and  $1B_g \leftarrow 1A_g$  transitions arising due to the promotion of electron from the doubly degenerate HOMO to the 3s Rydberg orbital  $(e_g \rightarrow 3s)$  of cyclohexane (shown in Figure 5). The  $e_g \rightarrow 3s$  type electron promotion is allowed in 2PA, but is extremely weak in 1PA, formally allowed only by vibronic coupling. This is consistent with the presence of a shoulder in the 2PA spectra at ~7.6 eV, while such a shoulder is not observed in the liquid 1PA spectra (Figure 3).

Natural transition orbital analysis reveals that, just like for cyclohexane, the strongest 2PA transitions for the TTT  $(4A_g \leftarrow 1A_g)$  and TGT  $(8A \leftarrow 1A)$  conformers of n-hexane also result from the electron promotion to the Rydberg 3d orbital. Similarly, the strongest transitions in 1PA are associated with electron promotion to the Rydberg 3p orbital:  $4B_u \leftarrow 1A_g$  for TTT and  $6B \leftarrow 1A$  for TGT conformer of n-hexane. It is interesting to note that the nature of the transition with the highest cross section in both 1PA and 2PA does not change between the highly symmetric cyclohexane

molecule ( $D_{3d}$  point group) and the TTT ( $C_{2h}$ ) and the TGT ( $C_2$ ) conformers of n-hexane which have lower symmetry. The change in molecular point group symmetry, however, impacts the transition strengths, as evident from the experimental 1PA and 2PA cross-sections and backed up by our EOM-CCSD calculations performed for both hexane isomers and cyclohexane.

#### VII. Conclusion

In this work, the broadband 2PA spectra of liquid cyclohexane and n-hexane have been reported for the first time. The experimental 2PA spectra are assigned and simulated using the transition energies and cross sections calculated for isolated cyclohexane and n-haxane molecules at EOM-CCSD/d-aug-cc-PVDZ level of theory. Simulation of liquid hexane spectra are performed for two different conformers of n-hexane (TTT and TGT) separately. To reproduce the general features of the experimental spectra, only minor modifications of the computed properties are necessary; our approach, while by necessity incomplete as to the condensed phase electronic structure, provide a reasonable starting point to assign the relatively featureless 2PA spectra and most importantly, the polarization ratio and suggest electron delocalization effects in the electronic structure must be small.

Cyclohexane is present predominantly in the chair conformation in the liquid phase at room temperature, and it belongs to highly symmetric  $D_{3d}$  point group with a center of inversion. The gas phase selection rule for this molecule dictates that the 1PA and 2PA active transitions are mutually exclusive. We find that the liquid phase 1PA and 2PA spectra can be reproduced surprisingly well by taking the gas phase 1PA and 2PA active transitions respectively as a basis and making relatively modest modifications to transition energies, but not transition strengths of the computed *in vacuo* properties. This emphasizes the fact that the gas phase selection rules are

still essentially valid in the liquid phase, and that electronic structure calculations for the isolated molecule form provide a reasonable starting point to analyze the liquid phase spectra.

For cyclohexane, transitions involving promotion of electrons to the 3s Rydberg orbitals are blueshifted by ~0.55 eV, while all other transitions appear to be less sensitive to the condensed environment. In n-hexane, the transitions involving the Rydberg 3s orbital are blue-shifted by ~0.18 eV while the remaining transitions are red-shifted by ~0.15-0.2 eV upon solvation. The smaller gas to liquid blueshift of the transitions to Rydberg 3s orbitals in n-hexane is attributed to lesser Pauli repulsion due to smaller size of the excited orbital and lower density of liquid hexane compared to that of liquid cyclohexane. The general red-shift of the higher order Rydberg transitions of n-hexane upon solvation is due to the greater stabilization of the cationic core.

The simulation of the liquid n-hexane spectra is difficult in comparison, since there are multiple conformers present in the liquid phase. Nevertheless, we simulated the hexane spectra using the theoretically computed properties for the TTT and TGT conformers. The TTT conformer has a center of inversion, but the TGT conformer does not. Therefore, all electronic states in the TGT conformer are active in both 1PA and 2PA spectroscopy. The simulation using *ab initio* results of the TGT conformer is in better accord with the experimental 2PA spectra compared to the TTT conformer, reflecting the presence of considerable amount of lower symmetry conformer in the liquid phase. Neither conformer alone can fully reproduce the experimental polarization ratio, although the presence of structural isomers in the experimental hexanes sample that including include methylcyclopentane may explain the discrepancy. These observations reinforce the idea that the polarization ratio is an extremely sensitive quantity in capturing the character of the electronic transitions in the 2PA spectra.

Our *ab initio* calculations and the NTO analysis reveal that the gas phase 1PA and 2PA transitions in hexane and cyclohexane are dominated by Rydberg excitations, even in the lowest energy region. These Rydberg transitions, understood and well-studied in the gas phase, are preserved in the liquid phase below the liquid phase ionization energy; the experimental 2PA spectra and the polarization ratio cannot be reproduced by removing these transitions from the simulation or assuming they are moved to much higher energy; likewise, no modifications to the oscillator strengths are required. These conclusions are similar to those made about the Rydberg spectrum for water and alcohols and reinforces the idea that electronic transitions in liquid phase can still be envisioned from a single-molecule framework and the gas phase transition properties are not substantially altered upon condensation.

## Supporting Information:

APA cross sections, 2PA cross sections, and polarization ratios of all calculated excited transitions for cyclohexane, TTT and TGT conformers of n-hexane are tabulated. The entire range of liquid 1PA spectrum of cyclohexane is shown. The section of the liquid 1PA spectrum of n-hexane is shown as well as simulations that do not include the imposition of solvent shifts discussed in the manuscripts and a deconstruction of the final Gaussian fit to the cyclohexane 2PA spectrum.

#### Acknowledgments:

This work was supported by the National Science Foundation (experimental work under CHE-0617060 and theoretical work under CHE-1665532). We thank Prof. Anna Krylov for helpful

Formatted: Font: 16 pt

Formatted: Line spacing: Double

Formatted: Font color: Text 1

Formatted: Font color: Dark Red

Formatted: Font: 16 pt

Formatted: Line spacing: Double

discussions regarding the calculation of two-photon properties. We also thank Shivalee Dey for giving critical inputs about the manuscript. We acknowledge the Center for High Performance Computing at the University of Southern California for supercomputer time allocation.

#### References

- 1. Reisler, H.; Krylov, A. I., Interacting Rydberg and Valence States in Radicals and Molecules: Experimental and Theoretical Studies. *International Reviews in Physical Chemistry* **2009**, *28*, 267-308.
- 2. Butler, L. J., Chemical Reaction Dynamics Beyond the Born-Oppenheimer Approximation. *Annual review of physical chemistry* **1998**, *49*, 125-171.
- 3. Worth, G. A.; Cederbaum, L. S., Beyond Born-Oppenheimer: Molecular Dynamics through a Conical Intersection. *Annu. Rev. Phys. Chem.* **2004**, *55*, 127-158.
- 4. Stolow, A., Femtosecond Time-Resolved Photoelectron Spectroscopy of Polyatomic Molecules. *Annual review of physical chemistry* **2003**, *54*, 89-119.
- 5. Stolow, A.; Bragg, A. E.; Neumark, D. M., Femtosecond Time-Resolved Photoelectron Spectroscopy. *Chemical reviews* **2004**, *104*, 1719-1758.
- 6. Stanton, J. F., Coupled-Cluster Theory, Pseudo-Jahn–Teller Effects and Conical Intersections. *The Journal of Chemical Physics* **2001**, *115*, 10382-10393.
- 7. Russ, N. J.; Crawford, T. D.; Tschumper, G. S., Real Versus Artifactual Symmetry-Breaking Effects in Hartree–Fock, Density-Functional, and Coupled-Cluster Methods. *The Journal of Chemical Physics* **2004**, *120*, 7298-7306.
- 8. Chergui, M.; Schwentner, N.; Tramer, A., Spectroscopy of the No Molecule in N2 and Mixed N2/Kr Matrices. *Chemical physics letters* **1993**, *201*, 187-193.
- 9. Vigliotti, F.; Chergui, M.; Dickgiesser, M.; Schwentner, N., Rydberg States in Quantum Crystals No in Solid H 2. *Faraday Discussions* **1997**, *108*, 139-159.
- 10. Chergui, M.; Schwentner, N.; Böhmer, W., Rydberg States of No Trapped in Rare Gas Matrices. *The Journal of Chemical Physics* **1986**, *85*, 2472-2482.
- 11. Chergui, M.; Schwentner, N.; Chandrasekharan, V., Rydberg Fluorescence of No Trapped in Rare Gas Matrices. *The Journal of Chemical Physics* **1988**, *89*, 1277-1284.
- 12. Vigliotti, F.; Chergui, M., Rydberg States in the Condensed Phase Studied by Fluorescence Depletion Spectroscopy. *The European Physical Journal D-Atomic, Molecular, Optical and Plasma Physics* **2000**, *10*, 379-390.
- 13. Scott, T. W.; Albrecht, A., A Rydberg Transition in Benzene in the Condensed Phase: Two-Photon Fluorescence Excitation Studies. *The Journal of Chemical Physics* **1981**, *74*, 3807-3812.
- 14. Vigliotti, F.; Zerza, G.; Chergui, M.; Rubayo-Soneira, J., Lifetime Lengthening of Molecular Rydberg States in the Condensed Phase. *The Journal of Chemical Physics* **1998**, *109*, 3508-3517.
- 15. Bernas, A.; Grand, D., The So-Called Ionization Potential of Water and Associated Liquids. *The Journal of Physical Chemistry* **1994**, *98*, 3440-3443.
- 16. Cheng, B.-M.; Bahou, M.; Chen, W.-C.; Yui, C.-h.; Lee, Y.-P.; Lee, L. C., Experimental and Theoretical Studies on Vacuum Ultraviolet Absorption Cross Sections and Photodissociation of Ch 3 Oh, Ch 3 Od, Cd 3 Oh, and Cd 3 Od. *The Journal of chemical physics* **2002**, *117*, 1633-1640.

Formatted: Font: 16 pt

- 17. Philis, J. G., Resonance-Enhanced Multiphoton Ionization Spectra of Jet-Cooled Methanol and Ethanol. *Chemical Physics Letters* **2007**, *449*, 291-295.
- 18. Bhattacharyya, D.; Zhang, Y.; Elles, C. G.; Bradforth, S. E., Electronic Structure of Liquid Methanol and Ethanol from Polarization-Dependent Two-Photon Absorption Spectroscopy. *The Journal of Physical Chemistry A* **2019**, *123*, 5789-5804.
- 19. Caldwell, J. W.; Gordon, M. S., Excited States and Photochemistry of Saturated Molecules. Minimal Plus Rydberg Basis Set Calculations on the Vertical Spectra of Ch4, C2h6, C3h8, and N-C4h10. *Chemical Physics Letters* **1978**, *59*, 403-409.
- 20. Lombos, B.; Sauvageau, P.; Sandorfy, C., The Electronic Spectra of N-Alkanes. *Journal of Molecular Spectroscopy* **1967**, *24*, 253-269.
- 21. Raymonda, J. W.; Simpson, W. T., Experimental and Theoretical Study of Sigma-Bond Electronic Transitions in Alkanes. *The Journal of Chemical Physics* **1967**. *47*. 430-448.
- 22. Raymonda, J. W., Rydberg States in Cyclic Alkanes. *The Journal of Chemical Physics* **1972**, *56*, 3912-3920.
- 23. Robin, M.; Basch, H.; Kuebler, N.; Wiberg, K.; Ellison, G., Optical Spectra of Small Rings. li. The Unsaturated Three-Membered Rings. *The Journal of Chemical Physics* **1969**, *51*, 45-52.
- 24. Shang, Q.; Bernstein, E., (Σ3 S) Rydberg States of Cyclohexane, Bicyclo [2.2. 2] Octane, and Adamantane. *The Journal of chemical physics* **1994**, *100*, 8625-8632.
- 25. Heath, B.; Kuebler, N.; Robin, M., Multiphoton Ionization Spectra of Polycyclic Alkanes. *The Journal of Chemical Physics* **1979**, *70*, 3362-3368.
- 26. Wagner, P.; Duncan, A., The Absorption Spectrum of Cyclopropane in the Vacuum Ultraviolet. Note on the Absorption Spectrum of Methyl Cyclopropane. *The Journal of Chemical Physics* **1953**, *21*, 516-519.
- 27. Robin, M. B., Higher Excited States of Polyatomic Molecules (Academic, New York, 1974). *Vol. I* **1975**, 180.
- 28. Anikeenko, A.; Kim, A.; Medvedev, N., Molecular Dynamics Simulation of the Structure of C6 Alkanes. *Journal of Structural Chemistry* **2010**, *51*, 1090-1096.
- 29. Gruzman, D.; Karton, A.; Martin, J. M., Performance of Ab Initio and Density Functional Methods for Conformational Equilibria of C N H2 N+ 2 Alkane Isomers (N= 4– 8). *The Journal of Physical Chemistry A* **2009**, *113*, 11974-11983.
- 30. Venturi, G.; Formisano, F.; Cuello, G.; Johnson, M.; Pellegrini, E.; Bafile, U.; Guarini, E., Structure of Liquid N-Hexane. *The Journal of chemical physics* **2009**, *131*, 034508.
- 31. Snyder, R. G.; Kim, Y., Conformation and Low-Frequency Isotropic Raman Spectra of the Liquid N-Alkanes C4-C9. *The Journal of Physical Chemistry* **1991**, *95*, 602-610.
- 32. Herzberg, G., *Electronic Spectra and Electronic Structure of Polyatomic Molecules*; van Nostrand, 1966; Vol. 3.
- 33. Wilson, E. B.; Decius, J. C.; Cross, P. C., Molecular Vibrations: The Theory of Infrared and Raman Vibrational Spectra; Courier Corporation, 1980.
- 34. Au, J. W.; Cooper, G.; Burton, G. R.; Olney, T. N.; Brion, C., The Valence Shell Photoabsorption of the Linear Alkanes, Cnh2n+ 2 (N= 1–8): Absolute Oscillator Strengths (7–220 Ev). *Chemical physics* **1993**, 173, 209-239
- 35. Tauber, M. J.; Mathies, R. A.; Chen, X.; Bradforth, S. E., Flowing Liquid Sample Jet for Resonance Raman and Ultrafast Optical Spectroscopy. *Review of scientific instruments* **2003**, *74*, 4958-4960.
- 36. Bartlett, R. J., The Coupled-Cluster Revolution. *Molecular Physics* **2010**, *108*, 2905-2920.
- 37. Stanton, J. F.; Bartlett, R. J., The Equation of Motion Coupled-Cluster Method. A Systematic Biorthogonal Approach to Molecular Excitation Energies, Transition Probabilities, and Excited State Properties. *The Journal of Chemical Physics* **1993**, *98*, 7029-7039.

- 38. Monson, P. R.; McClain, W. M., Polarization Dependence of the Two-Photon Absorption of Tumbling Molecules with Application to Liquid 1-Chloronaphthalene and Benzene. *The Journal of Chemical Physics* **1970**, *53*, 29-37.
- 39. Nanda, K. D.; Krylov, A. I., Two-Photon Absorption Cross Sections within Equation-of-Motion Coupled-Cluster Formalism Using Resolution-of-the-Identity and Cholesky Decomposition Representations: Theory, Implementation, and Benchmarks. *The Journal of chemical physics* **2015**, *142*, 064118.
- 40. McClain, W. M., Excited State Symmetry Assignment through Polarized Two-Photon Absorption Studies of Fluids. *The Journal of Chemical Physics* **1971**, *55*, 2789-2796.
- 41. McClain, W. M., Two-Photon Molecular Spectroscopy. *Accounts of Chemical Research* **1974**, *7*, 129-135.
- 42. Monson, P.; McClain, W., Complete Polarization Study of the Two-Photon Absorption of Liquid 1-Chloronaphthalene. *The Journal of Chemical Physics* **1972**, *56*, 4817-4825.
- 43. Elles, C. G.; Rivera, C. A.; Zhang, Y.; Pieniazek, P. A.; Bradforth, S. E., Electronic Structure of Liquid Water from Polarization-Dependent Two-Photon Absorption Spectroscopy. *The journal of chemical physics* **2009**, *130*, 084501.
- 44. Chen, J.; Ping, J.; Wang, F., Representation Theory for Physicists, World Sci. Publ. Co., MA 2002.
- 45. De Wergifosse, M.; Houk, A. L.; Krylov, A. I.; Elles, C. G., Two-Photon Absorption Spectroscopy of Trans-Stilbene, Cis-Stilbene, and Phenanthrene: Theory and Experiment. *The Journal of Chemical Physics* **2017**, *146*, 144305.
- 46. Jung, J.; Gress, H., Single-Photon Absorption of Liquid Cyclohexane, 2, 2, 4 Trimethylpentane and Tetramethylsilane in the Vacuum Ultraviolet. *Chemical physics letters* **2003**, *377*, 495-500.
- 47. Costner, E. A.; Long, B. K.; Navar, C.; Jockusch, S.; Lei, X.; Zimmerman, P.; Campion, A.; Turro, N. J.; Willson, C. G., Fundamental Optical Properties of Linear and Cyclic Alkanes: Vuv Absorbance and Index of Refraction. *The Journal of Physical Chemistry A* **2009**, *113*, 9337-9347.
- 48. Tachibana, S.; Morisawa, Y.; Ikehata, A.; Sato, H.; Higashi, N.; Ozaki, Y., Far-Ultraviolet Spectra of N-Alkanes and Branched Alkanes in the Liquid Phase Observed Using an Attenuated Total Reflection–Far Ultraviolet (Atr-Fuv) Spectrometer. *Applied Spectroscopy* **2011**, *65*, 221-226.
- 49. Morisawa, Y.; Ikehata, A.; Higashi, N.; Ozaki, Y., Attenuated Total Reflectance—Far Ultraviolet (Atr—Fuv) Spectra of Ch3oh, Ch3od, Cd3oh and Cd3od in a Liquid Phase~ Rydberg States~. *Chemical Physics Letters* **2009**, *476*, 205-208.
- 50. Siebbeles, L. D.; Emmerichs, U.; Hummel, A.; Bakker, H. J., A Subpicosecond Pump-Probe Laser Study of Ionization and Geminate Charge Recombination Kinetics in Alkane Liquids. *The Journal of chemical physics* **1997**, *107*, 9339-9347.
- 51. Shida, T.; Takemura, Y., Electronic Absorption Spectra of Cation-Radicals of Alkanes and Ccl4 by a Combined Optical and Esr Studies for Γ-Irradiated Rigid Solutions. *Radiation Physics and Chemistry* (1977) **1983**. 21. 157-166.
- 52. Tagawa, S.; Hayashi, N.; Yoshida, Y.; Washio, M.; Tabata, Y., Pulse Radiolysis Studies on Liquid Alkanes and Related Polymers. *International Journal of Radiation Applications and Instrumentation. Part C. Radiation Physics and Chemistry* **1989**, *34*, 503-511.
- 53. Larsen, H.; Hald, K.; Olsen, J.; Jørgensen, P., Triplet Excitation Energies in Full Configuration Interaction and Coupled-Cluster Theory. *The Journal of Chemical Physics* **2001**, *115*, 3015-3020.
- 54. Zuev, D.; Bravaya, K. B.; Crawford, T. D.; Lindh, R.; Krylov, A. I., Electronic Structure of the Two Isomers of the Anionic Form of P-Coumaric Acid Chromophore. *The Journal of chemical physics* **2011**, *134*, 034310.
- 55. Epifanovsky, E.; Kowalski, K.; Fan, P.-D.; Valiev, M.; Matsika, S.; Krylov, A. I., On the Electronically Excited States of Uracil. *The Journal of Physical Chemistry A* **2008**, *112*, 9983-9992.

- 56. Loos, P.-F.; Boggio-Pasqua, M.; Scemama, A.; Caffarel, M.; Jacquemin, D., Reference Energies for Double Excitations. *Journal of chemical theory and computation* **2019**, *15*, 1939-1956.
- 57. Bhattacharyya, D.; Mizuno, H.; Rizzuto, A. M.; Zhang, Y.; Saykally, R. J.; Bradforth, S. E., New Insights into the Charge-Transfer-to-Solvent Spectrum of Aqueous Iodide: Surface Versus Bulk. *The journal of physical chemistry letters* **2020**, *11*, 1656-1661.
- 58. Bravaya, K. B.; Krylov, A. I., On the Photodetachment from the Green Fluorescent Protein Chromophore. *The Journal of Physical Chemistry A* **2013**, *117*, 11815-11822.
- 59. Marenich, A. V.; Cramer, C. J.; Truhlar, D. G., Uniform Treatment of Solute–Solvent Dispersion in the Ground and Excited Electronic States of the Solute Based on a Solvation Model with State-Specific Polarizability. *Journal of chemical theory and computation* **2013**, *9*, 3649-3659.
- 60. Roesch, N.; Zerner, M. C., Calculation of Dispersion Energy Shifts in Molecular Electronic Spectra. *The Journal of Physical Chemistry* **1994**, *98*, 5817-5823.
- 61. Iwahashi, M.; Kasahara, Y., Effects of Molecular Size and Structure on Self-Diffusion Coefficient and Viscosity for Saturated Hydrocarbons Having Six Carbon Atoms. *Journal of oleo science* **2007**, *56*, 443-448.
- 62. Bosque, R.; Sales, J., Polarizabilities of Solvents from the Chemical Composition. *Journal of chemical information and computer sciences* **2002**, *42*, 1154-1163.

# TOC graphic:

